Bull. Mater. Sci. (2019) 42:233
https://doi.org/10.1007/s12034-019-1916-z

Removal of hexavalent chromium from aqueous solutions using Ni–SiO_2 nanomaterials

HADI M MARWANI[1,2,*], EKRAM Y DANISH[1], KHOLOUD F ALMOSLEHI[1], SHER BAHADAR KHAN[1,2], ESRAA M BAKHSH[1] and ABDULLAH M ASIRI[1,2]

[1]Department of Chemistry, Faculty of Science, King Abdulaziz University, P.O. Box 80203, Jeddah 21589, Saudi Arabia
[2]Center of Excellence for Advanced Materials Research (CEAMR), King Abdulaziz University, P.O. Box 80203, Jeddah 21589, Saudi Arabia
*Author for correspondence (hmarwani@kau.edu.sa)

MS received 7 December 2018; accepted 21 April 2019

Abstract. This study describes an effective method developed for the removal of hexavalent chromium, Cr(VI), from an aqueous environment. In this study, the Ni–SiO_2 nanomaterial was synthesized by the sol–gel method and then characterized by field emission scanning electron microscopy, X-ray diffraction and energy dispersive X-ray spectroscopy. The prepared nanomaterial was then employed as an adsorbent with significant properties of high surface area and uptake capacity. Adsorption conditions of Cr(VI) onto the Ni–SiO_2 nanomaterial were optimized by altering different parameters (pH, initial Cr(VI) concentration and different periods of time). An amount of 100.75 mg g^{-1} was estimated as the maximum uptake capacity of the Ni–SiO_2 nanomaterial at pH 4.0. The experimental data of Cr(VI) adsorption onto the Ni–SiO_2 nanomaterial were fitted well to the Langmuir isotherm and pseudo second-order kinetic models. Moreover, the adsorption of Cr(VI) onto the Ni–SiO_2 nanomaterial was not influenced even in the presence of different coexisting ions. Finally, the recommended methodology was applied on several environmental water samples.

Keywords. Chromium; Ni–SiO_2; nanomaterials; selectivity; adsorption capacity; environmental applications.

1. Introduction

Chromium is one of the heavy metals that constituted threats to the environment. The trivalent, Cr(III), and hexavalent, Cr(VI), forms of chromium are the most abundant oxidation states in wastewater. Cr(VI) and its compounds are considered more toxic than Cr(III), where they have mutagenic and carcinogenic effects and also cause ulceration, liver damage, congestion, pulmonary, vomiting and skin irritation, unlike Cr(III) which is considered as an essential micronutrient at low levels [1–4]. Many industries—such as textile colouring, paint manufacturing, metal polishing, electroplating and leather tanning—contribute to the discharge of high concentrations of Cr(VI) to the environment, while the allowable concentration for Cr(VI) in potable water is only 0.05 and 0.1 mg l^{-1} into the inland surface water [5–7]. Therefore, it is of importance to remove or reduce Cr(VI) concentrations to permissible limit levels using selective techniques.

Various techniques were developed for the separation and removal of Cr(VI) from aqueous media including electrodialysis [8], membrane separation [9], chemical reduction/precipitation [10], ion exchange [11] and adsorption [12]. However, there are some disadvantages associated with precipitation and the most prominent is the large consumption of reagents [13]. Also, electrodialysis, membrane processes and ion exchange are not economical due to their high operational costs [14]. Among these techniques, adsorption onto the solid phase has attracted attention due to its efficiency, facility of operation and low-cost compared with other techniques. Nevertheless, the most important step to ensure high adsorption capacity is selecting the appropriate adsorbent. There are several adsorbents that are commonly used for Cr(VI) extraction such as activated carbon [15], alumina [16] and biomaterials [17].

Recently, intensive studies have been performed to utilize nanosized materials in the development of new methods to efficiently detect and remove heavy metals with high selectivity. Nanostructured materials exhibit unparalleled aptitudes as adsorbents for the extraction and separation of metal ions [18–22]. In addition, nanomaterials have particular shapes, are small in size, have extraordinary surface activity and also a high active surface-to-volume ratio, which generate and enhance different properties [23–26]. It is well-known that nanosized-materials are used perfectly in many applications; however, adsorption applications still require reformation of such nanomaterials to enhance its properties. Among different improvement techniques, doping of nanomaterials is a well-known approach to modulate the outstanding characteristics of nanoparticles. Dopants increase the surface area, reduce the mass and alter the morphologies of the nanomaterials resulting in the much-improved properties of nanomaterials [27–29].

Published online: 16 July 2019

Diverse nanosized-adsorbents have been reported for the removal of Cr(VI) from aqueous media. In the literature, metal oxide nanoparticles, especially, magnetic nanoparticles have been successfully applied for Cr(VI) adsorption with and without embedment in polymeric matrices [30,31]. More recently, zero-valent metal nanoparticle-supported appropriate materials have become important adsorbents for the extractive removal of Cr(VI) from water samples [32,33]. The use of layered double hydroxide materials and their composites was also reported as efficient adsorbents for Cr(VI) [34,35].

In this research, a nanomaterial composed of Ni-doped SiO_2 was prepared and used as an adsorbent to extract Cr(VI) from aquatic solutions. The selectivity of the Ni–SiO_2 nanomaterial was studied toward several metals, including Au(III), Co(II), Cd(II), Zn(II), Pd(II), Cr(III) and Cr(VI), to evaluate its efficacy on the extraction of selected metals. The Ni–SiO_2 nanomaterial achieved the utmost selectivity toward Cr(VI). Therefore, Cr(VI) has been selected to accomplish the study by investigating the different parameters that may affect the adsorption process performance. In addition, experimental data for Cr(VI) adsorption on the Ni–SiO_2 nanomaterial were modelled using different adsorption isotherm and kinetic models. This methodology was ultimately applied on real water samples.

2. Experimental

2.1 *Materials*

Tetraethoxysilane (TEOS, $Si(OC_2H_5)_4$) hexahydrated nickel nitrate $Ni(NO_3)_2 \cdot 6H_2O$, cetyltrimethylammonium bromide (CTAB) $[(C_{16}H_{33})N(CH_3)_3]$, ethanol, ammonia NH_4OH and 1000 mg l^{-1} stock standard solutions for each of Au(III), Co(II), Cd(II), Zn(II), Pd(II), Cr(III) and Cr(VI) were purchased from Sigma-Aldrich. Doubly distilled deionized water and high purity reagents were used throughout the experiments.

2.2 *Preparation of Ni–SiO_2 nanomaterial*

The Ni–SiO_2 nanomaterial was prepared by the sol–gel method [36]. The required amount of $Ni(NO_3)_2 \cdot 6H_2O$ was added to a conical flask charged with water (20 ml), ethanol (80 ml) and CTAB (0.6 g) and then, concentrated ammonia solution (1 g, 4 ml, 28 wt%) was added and the mixture was well dispersed. After dispersion, 0.4 g of TEOS was added dropwise and the reaction was allowed to proceed overnight under continuous mechanical stirring. The resulting product was washed with distilled water and ethanol (1:1) and dried at 50°C.

2.3 *Sample preparation and adsorption experiments*

Standard solutions of 5 mg l^{-1} for selected metal ions were prepared and then mixed separately with 10 mg of the Ni–SiO_2 nanomaterial to study the selectivity of the Ni–SiO_2 nanomaterial toward these metal ions. All mixtures were shaken mechanically for an hour at 25°C. Metal ion concentrations were measured after filtration immediately by inductively coupled plasma-optical emission spectrometry (ICP-OES) at the wavelengths of 276.595, 228.616, 228.802, 206.200, 324.270, 267.716 and 267.716 nm for Au(III), Co(II), Cd(II), Zn(II), Pd(II), Cr(III) and Cr(VI), respectively. Then, the effects of solution pH, initial concentration, contact time and coexisting ions were studied for the most selective metal ion, which is Cr(VI), under static conditions. To study the effect of pH on Cr(VI) extraction using the Ni–SiO_2 nanomaterial, 5 mg l^{-1} standard solutions were adjusted by buffer solutions in the pH range of 1–9, 0.2 mol l^{-1} HCl/KCl for pH 1 and 2, 0.1 mol l^{-1} CH_3COOH/CH_3COONa for pH 3–6, and 0.1 mol l^{-1} Na_2HPO_4/HCl for pH 7–9, further, individually mixed with 10 mg Ni–SiO_2. These mixtures were also shaken mechanically for an hour at 25°C. To determine the adsorption capacity of Cr(VI), standard solutions of 5, 10, 15, 25, 35, 50, 75, 100, 125, 150, 200, 300, 400 and 500 mg l^{-1} of Cr(VI) were prepared at an optimum value of pH 4. Moreover, contact time influence on Cr(VI) uptake capacity by the Ni–SiO_2 nanomaterial was studied at 25°C and pH 4 for different periods of time (2, 5, 10, 20, 30, 40, 50 and 60 min).

3. Results and discussion

3.1 *Characterization of Ni–SiO_2 nanomaterial*

Field emission scanning electron microscopy (FESEM) images (figure 1a) were analysed for the morphology of the Ni–SiO_2 nanomaterial which shows that the Ni–SiO_2 nanomaterial was prepared in the form of spheres and the as-grown spheres of Ni–SiO_2 are composed of nanoparticles. Thus, Ni–SiO_2 is initially grown as particles and then the nanoparticles get aggregated and form a sphere-like structure.

Ni–SiO_2 is further characterized by using transmission electron microscopy (TEM) and the images are shown in figure 1b. TEM analysis also shows a sphere-like structure with a size of <1 μm. These spheres contain nanosized particles. These nanosized particles aggregate together in such a way to form spherical structures.

Figure 2 shows the X-ray diffraction (XRD) pattern of the Ni–SiO_2 nanomaterial. Ni diffraction peaks and SiO_2 diffraction peaks are clearly observed, indicating the successful preparation of the Ni–SiO_2 nanomaterial. The broad hump at around 23° is due to the amorphous SiO_2 phase, while the peak at 44° appeared due to the presence of Ni. The XRD data exactly match with the peaks related to the SiO_2 and Ni pattern in the literature [36–38].

The elemental composition of the Ni–SiO_2 nanomaterial was determined using energy dispersive X-ray spectroscopy (EDS). The EDS spectrum (figure 3) showed peaks for Ni, Si, C and O which confirm the formation of the Ni–SiO_2

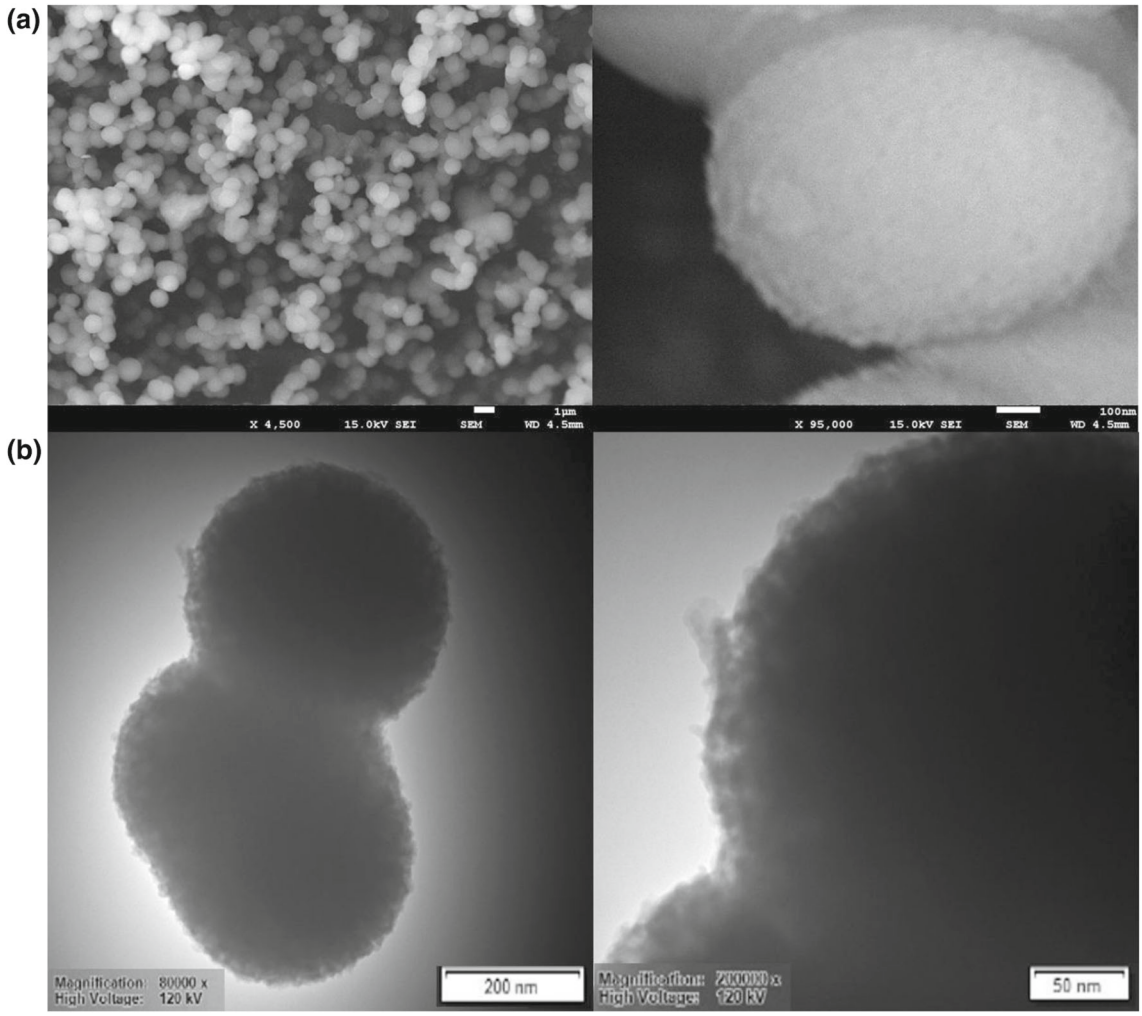

Figure 1. (**a**) FESEM and (**b**) TEM images of the Ni–SiO_2 nanomaterial.

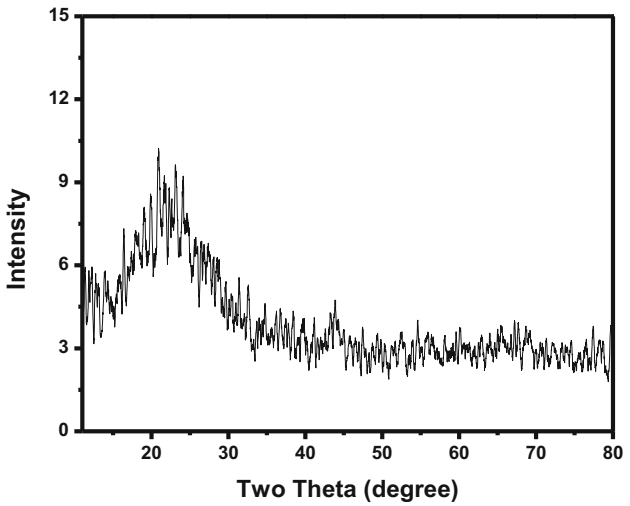

Figure 2. XRD pattern of the Ni–SiO_2 nanomaterial.

nanomaterial, whereas the appearance of the carbon peak is owing to the surfactant used during the preparation of the nanoparticles.

The surface area is an important parameter of nanomaterials which can determine the adsorption capacity of any material toward metal ions. The adsorption capacity of Cr(IV) on Ni–SiO_2 is a critical step in adsorption which is determined from the surface area of Ni–SiO_2. Quantachrome Instruments (version 2.2) were used to measure the surface area of Ni–SiO_2 and the adsorption–desorption isotherm is shown in figure 4. The shape of the adsorption–desorption isotherm for Ni–SiO_2 indicates a V-type isotherm. The surface area, pore volume and pore diameter of Ni–SiO_2 during the adsorption and desorption process are given in table 1, which confirmed the standard values (1.5–100 nm). The linearity of the data over the relative pressure (P/P_0) range 0.1–0.4 suggests the suitability of the Brunauer–Emmett–Teller (BET) model to determine the surface area of Ni–SiO_2.

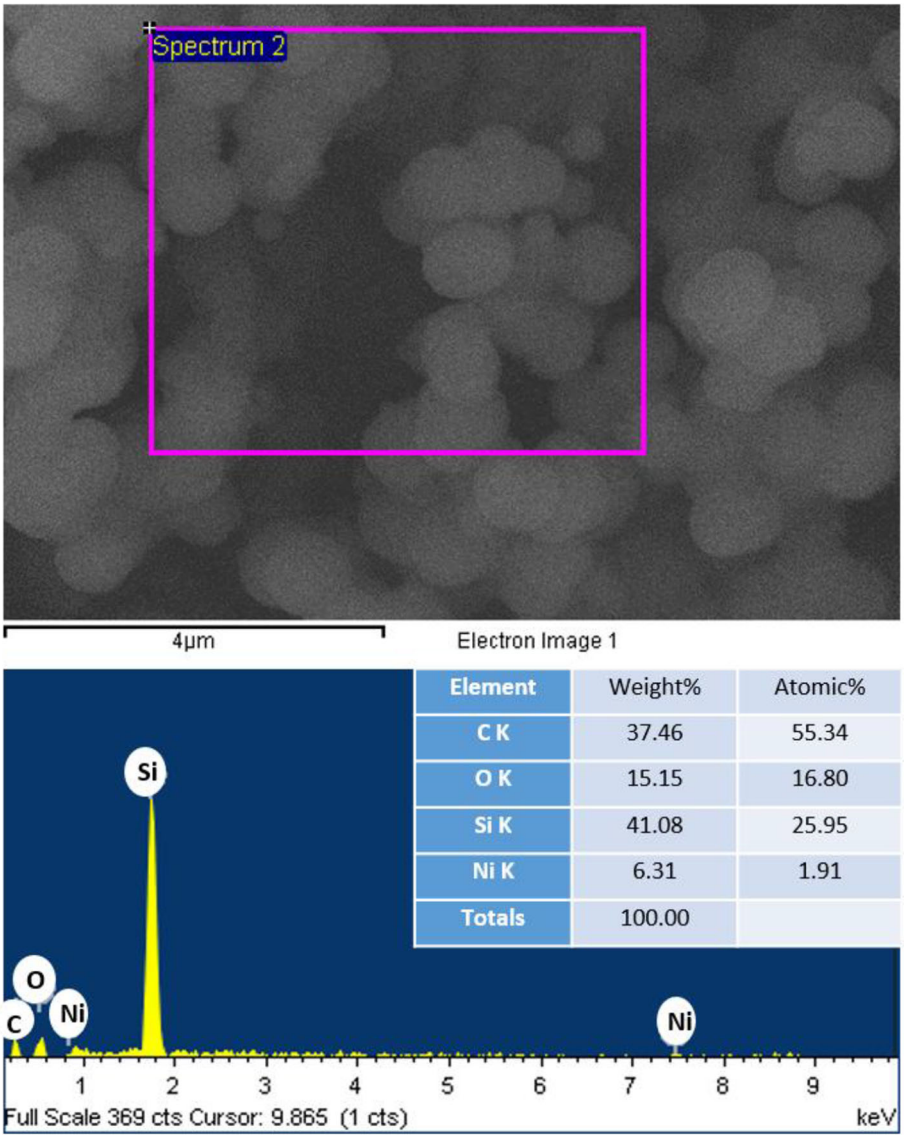

Figure 3. EDS of the Ni–SiO_2 nanomaterial.

3.2 *Adsorption of Cr(VI)*

3.2a *Selectivity study*: The selectivity of the Ni–SiO_2 nanomaterial toward selected metal ions was examined on the basis of the distribution coefficient determination, which corresponds to the character of the analyte adsorbed by an adsorbent. The distribution coefficient (K_d) and the amount adsorbed per unit mass of the adsorbent at equilibrium (q_e) were obtained by the following equations [39]:

$$K_d = \frac{(C_o - C_e)}{C_e} \times \frac{V}{m}, \tag{1}$$

$$q_e = \frac{(C_o - C_e)V}{m}, \tag{2}$$

where C_o and C_e refer to the initial and the final concentrations of the metal ion, respectively, m refers to the Ni–SiO_2 nanomaterial weight (g) and V is the volume (ml) of the sample. The values of the distribution coefficients of metal ions, mentioned in the experimental part, are listed in table 2. The results indicated that the highest value of K_d was for Cr(VI), 165,510.75 ml g^{-1}, on the Ni–SiO_2 nanomaterial among all other metal ions, which means that the Ni–SiO_2 nanomaterial was most selective toward Cr(VI). This ascribed to the more negative charges possessed by Cr(VI) compared with other studied metals, which are easily attracted to nickel dopants on the adsorbent surface.

3.2b *Effect of pH*: The most critical parameter that affects Cr(VI) adsorption onto the Ni–SiO_2 nanomaterial surface is solution pH which controls the adsorbent surface charge and also impacts the metal ion speciation. To investigate the pH

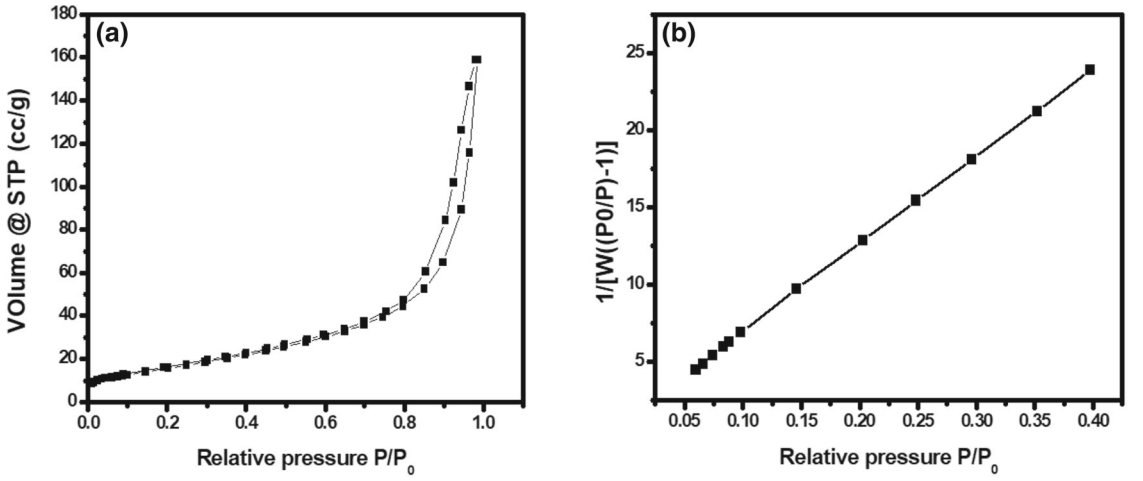

Figure 4. (**a**) BET N_2 adsorption–desorption isotherm and (**b**) the multipoint BET plot for the Ni–SiO_2 nanomaterial.

Table 1. Parameters calculated from BET N_2 adsorption–desorption isotherm of the Ni–SiO_2 nanomaterial.

Analysis	Surface area ($m^2\ g^{-1}$)	Pore volume ($cm^3\ g^{-1}$)	Pore diameter $Dv(d)$ (nm)
Adsorption	53.001	0.240	3.052
Desorption	57.535	0.241	3.827

Table 2. Selectivity study of Ni–SiO_2 nanomaterial adsorption toward different metal ions at 25°C.

Metal ion	Uptake capacity (mg g^{-1}), q_e	Distribution coefficient (ml g^{-1}), K_d
Cr(VI)	12.31	165,510.75
Au(III)	5.79	2157.23
Pd(II)	3.41	935.95
Co(II)	2.20	533.98
Cd(II)	1.95	462.09
Cr(III)	1.83	427.40
Zn(II)	1.48	335.75

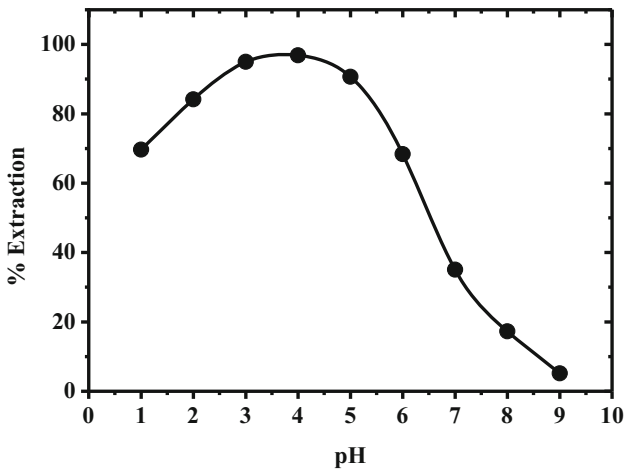

Figure 5. Effect of pH on 5 mg l^{-1} Cr(VI) adsorption on 10 mg Ni–SiO_2 nanomaterial at 25°C.

effect on the Ni–SiO_2 nanomaterial affinity toward Cr(VI), different pH media of sample solutions were investigated through preparing Cr(VI) standard solutions with pH values ranging from 1 to 9 and then individually mixing with 10 mg Ni–SiO_2 nanomaterials and shaking mechanically for an hour at room temperature. From figure 5, it is obvious that the percentage of extraction largely depends on the pH of the solution since it increased with increasing pH from 1 to 4, then decreased gradually thereafter. Also, figure 5 illustrates that the Cr(VI) extraction percentage reached the highest value (96.84%) at pH 4, which indicates that the Ni–SiO_2 nanomaterial was most selective toward Cr(VI) at this pH. The extraction percentage of Cr(VI) was calculated by the following equation:

$$\%\ \text{extraction} = \frac{C_o - C_e}{C_o} \times 100. \tag{3}$$

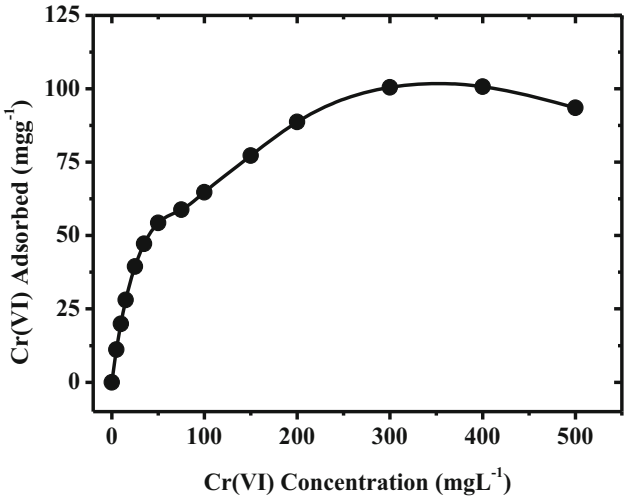

Figure 6. Effect of the Cr(VI) concentration on the adsorption process by 10 mg Ni–SiO_2 nanomaterial at pH 4 and 25°C.

In fact, Cr(VI) ions predominantly existed in the form of $HCrO_4^-$ at a pH range of 2–5, which have the ability to bond with positively charged functional groups easily through electrostatic attraction. At pH > 5, the concentration of CrO_4^{-2} increased progressively with the increasing pH of the solution. Under these conditions, the percentage extraction of Cr(VI) decreased gradually until it reached a pH of 9. Moreover, the existing anions in the sample solution may compete with the Cr(VI) species to bind the surface of the Ni–SiO_2 nanomaterial by increasing the pH of the solution [40,41]. Thus, we can conclude from the pH study that at pH around 5, a strong interaction between the $HCrO_4^-$ species and nickel dopants on the adsorbent surface has occurred, leading to the high extraction percentage of Cr(VI) from the solution. Several studies were reported at pH 4–5 as the optimum condition for Cr(VI) adsorption [42], which matched with the obtained results in the current study.

3.2c *Adsorption capacity determination*: For estimating the uptake capacity of the Ni–SiO_2 nanomaterial, a series of samples with a volume of 25 ml and the concentrations varied from 0 to 500 mg l^{-1} of Cr(VI) were prepared at pH 4. Then, the separation procedure previously mentioned above was applied to these solutions. Then, the amount of Cr(VI) adsorbed was measured at each concentration level using ICP-OES. The profile of Cr(VI) adsorption on the 10 mg Ni–SiO_2 nanomaterial was obtained by plotting Cr(VI) concentrations (mg l^{-1}) against the adsorbed amount of Cr(VI) on the Ni–SiO_2 nanomaterial (mg g^{-1}) (figure 6). The adsorption capacity of the Ni–SiO_2 nanomaterial for Cr(VI) experimentally obtained from the study, was calculated to be 100.75 mg g^{-1} (figure 6), which is comparable with other materials recently mentioned for Cr(VI) uptake by different researchers (table 3) [40,42–50].

3.2d *Adsorption isotherm models*: Freundlich and Langmuir isotherm models were employed for the analysis, explaining the isotherm equilibrium data [51,52]. The results demonstrated that the experimental data fitted well with the Langmuir equation, which assumes that a monolayer adsorption takes place on a surface containing an adsorption site with finite number and uniform energies of adsorption. The Langmuir isotherm model is described as follows [53]:

$$C_e/q_e = (C_e/Q_o) + 1/Q_o b, \tag{4}$$

where C_e is the metal ion concentration at equilibrium (mg l^{-1}), q_e is the adsorbed amount of the metal ion at equilibrium (mg g^{-1}) and Q_o and b are Langmuir constants. Since Q_o is the maximum capacity of Cr(VI) adsorption (mg g^{-1}) and b is the affinity parameter (l mg^{-1}), Q_o and b are calculated from the linear plot of C_e *vs.* C_e/q_e with an intercept of $(1/Q_o b)$ and slope of $(1/Q_o)$.

A dimensionless constant separation factor or equilibrium parameter (R_L) can be utilized to describe the nature of the adsorption isotherm. Values between 0 and 1 indicate a favourable adsorption, and it can be calculated by the following equation [54]:

$$R_L = \frac{1}{(1 + bC_o)}, \tag{5}$$

where C_o denotes the initial concentration of the metal ion and b is the Langmuir constant that indicates the shape of the isotherm and the nature of adsorption.

Figure 7 confirms the validity of the Langmuir isotherm model for the adsorption, which means that the adsorption was fundamentally a monolayer on a homogeneous adsorbent surface. The value of the correlation coefficient calculated from the Langmuir equation was $R^2 = 0.99$, indicating that the data were completely favourable with the Langmuir model. Q_o and b were determined to be 100.51 mg g^{-1} and 0.0524 l mg^{-1}, respectively. The obtained R_L value of Cr(VI) adsorption onto the Ni–SiO_2 nanomaterial was 0.05, which accentuates a well opportune adsorption to the Langmuir isotherm model.

3.2e *Effect of contact time*: To determine the probable order and required time for reaching the equilibrium of Cr(VI) adsorption onto a Ni–SiO_2 nanomaterial, the influence of contact time on the amount of extracted Cr(VI) was studied at a period of time ranging from 2 to 60 min for 400 mg l^{-1} of Cr(VI). The Cr(VI) amount adsorbed onto the Ni–SiO_2 nanomaterial increased on increasing the shaking time, which pointed out that the Ni–SiO_2 nanomaterial had fast adsorption kinetics for Cr(VI) (figure 8). Also, figure 8 obviously showed that up to 79.75 mg g^{-1} of Cr(VI) was adsorbed onto the Ni–SiO_2 nanomaterial after 20 min of the equilibrium period, while after 40 min, the amount adsorbed was increased to > 88 mg g^{-1}, and finally, Cr(VI) adsorption onto the Ni–SiO_2

Table 3. Comparison of Ni–SiO_2 nanomaterial adsorption capacity for Cr(VI) in the present study with other approaches recently reported.

Adsorbent	pH	q_e (mg g^{-1})	Reference
$(NH_2$–TNTs)[a]	4.5	153.85	[40]
MoS_2@(Fe_3O_4 NPs)[b]	5	218.18	[42]
$AlPO_4$-modified biosynthetic Schwertmannite	5	38.82	[43]
Natural Akadama clay	2	4.29	[44]
Amine-functionalized (MRS)[c]	2	15.82	[45]
(M-MWCNT)[d]	—	14.28	[46]
Chitosan/(PMMA)[e]composite nanofibrous membrane	3	92.5	[47]
(Cr(VI)–MIIP)[f]	3	39.3	[48]
(AC–TRIS)[g]	1	43.30	[49]
(OTA)[h]	1	95.9	[50]
Ni–SiO_2 nanomaterial	4	100.75	This study

[a]Amino-functionalized titanate nanotubes.
[b]Magnetic Fe_3O_4 nanoparticles decorated with MoS_2.
[c]Modified-rice straw.
[d]Modified-multi-walled carbon nanotubes.
[e]Polymethylmethacrylate.
[f]Magnetic Cr(VI) ion imprinted polymer.
[g]Activated carbon modified with tris(hydroxymethyl)aminomethane.
[h]*Ocimum tenuiflorum*.

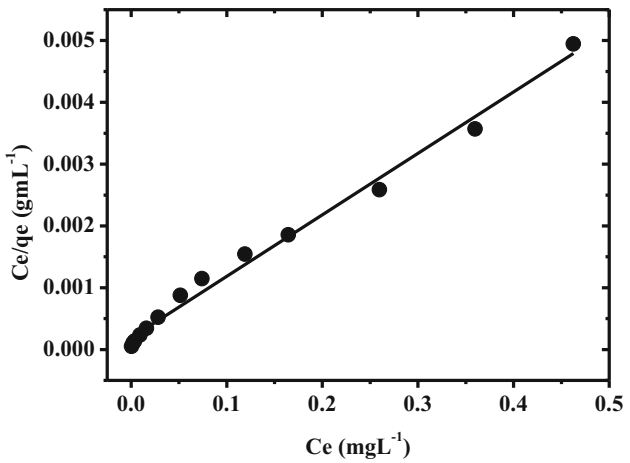

Figure 7. Langmuir adsorption isotherm of Cr(VI) adsorption on 10 mg Ni–SiO_2 nanomaterial at pH 4, 25°C and Cr(VI) concentrations (0–500 mg l^{-1}).

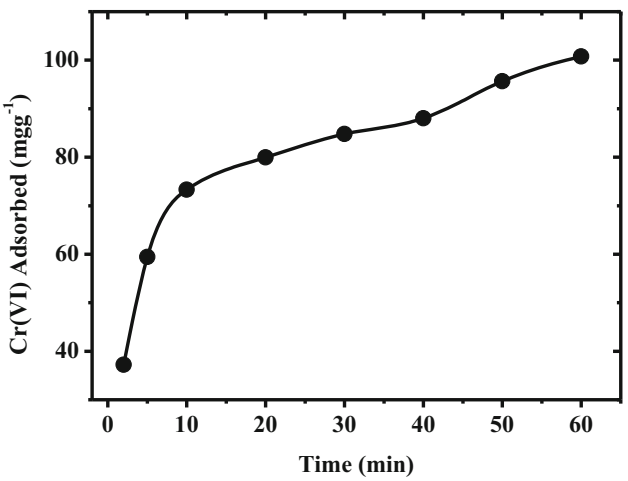

Figure 8. Effect of the contact time on the adsorption of 400 mg l^{-1} Cr(VI) on 10 mg Ni–SiO_2 nanomaterial at pH 4 and 25°C.

nanomaterial reached the maximum amount (100.75 mg g^{-1}) at 60 min of contact time.

3.2f *Kinetic isotherm models*: The study of adsorption kinetics is important to explain the reaction mechanism. Therefore, the Cr(VI) adsorption process onto the Ni–SiO_2 nanomaterial was studied by various adsorption kinetic models. These models were used with the experimental data to determine whether the experimental data are consistent with the calculated data utilizing the correlation coefficient (R^2). It should be noted that the kinetics data of adsorption were exceedingly compatible with the pseudo-second-order model, which was expressed as follows:

$$t/q_t = 1/\upsilon_o + (1/q_e)\,t, \tag{6}$$

where $\upsilon_o = k_2 q_e^2$ (mg g^{-1} min^{-1}) denotes the initial adsorption rate, k_2 (g mg^{-1} min^{-1}) is the adsorption rate constant, q_t and q_e (mg g^{-1}) are the adsorbed amount of the metal ion at any time t (min) and equilibrium, respectively, and q_e and υ_o parameters can be calculated by plotting t/q_t *vs.* t, where q_e and υ_o could be obtained from the slope and

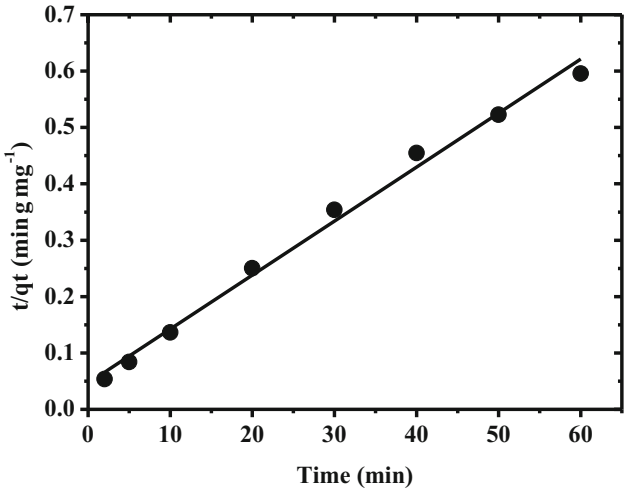

Figure 9. Pseudo-second-order kinetic model for Cr(VI) adsorption on 10 mg Ni–SiO_2 nanomaterial at pH 4 and 25°C.

intercept (figure 9). The pseudo-second-order model assumes that the rate-limiting step could be chemical adsorption involving valence forces through the exchange or sharing of electrons between the adsorbate and the adsorbent [54,55].

The R^2 value was found to be 0.993 which proved that the pseudo-second-order model is reliable and most accurate than other models. The parameters q_e, υ_o and k_2 were determined as 104.36 mg g^{-1}, 21.53 mg g^{-1} min^{-1} and 0.002 g mg^{-1} min^{-1}, respectively. Based on the pseudo-second-order kinetic model, the adsorption capacity of Cr(VI) onto the Ni–SiO_2 nanomaterial was calculated as 93.24 mg g^{-1}. Interestingly, the adsorption capacity of Cr(VI) onto the Ni–SiO_2 nanomaterial acquired from the pseudo-second-order kinetic model was agreed well with the capacity values obtained from both the Langmuir isotherm model (100.51 mg g^{-1}) and adsorption isotherm experiments (100.75 mg g^{-1}), indicating the validity of this model for interpreting adsorption kinetics.

3.3 *Performance of suggested procedure*

3.3a *Effect of coexisting ions*: The applicability of the designed procedure for analytical applications was investigated by evaluating the effect of the coexisting ions on Cr(VI) extraction. Standard solutions containing 3 mg l^{-1} Cr(VI) mixed with matrix ions were treated based on the suggested method, and table 4 summarizes the results. The results disclosed that Cr(VI) adsorption was not influenced by the medium composition containing mixed or individual ions. This behaviour ascribed to the low-rate or capacity of adsorption for other ions toward the Ni–SiO_2 nanomaterial. Thus, the results indicated that the Ni–SiO_2 nanomaterial has high selectivity toward Cr(VI) compared with other coexisting ions, and therefore, the suggested procedure can be applied for Cr(VI) extraction from real samples.

Table 4. Effect of matrix interferences on the extraction of 3 mg l^{-1} Cr(VI) on 10 mg Ni–SiO_2 nanomaterial.

Coexisting ions	Concentration (mg l^{-1})	Extraction % of Cr(VI)
Na^+, K^+, NH_4^+	9000	99.22
Ca^{2+}, Mg^{2+}	9000	98.61
Cd^{2+}	600	98.23
Co^{2+}	600	97.76
Cu^{2+}	600	98.12
Ni^{2+}	600	96.35
Zn^{2+}	600	97.58
Al^{3+}	300	94.63
Fe^{3+}	300	95.74
Cl^-, F^-, NO_3^-	3000	98.01
CO_3^{2-}, SO_4^{2-}	3000	97.75
PO_4^{3-}	3000	97.34

Table 5. Determination of Cr(VI) at different concentrations in real water samples using 10 mg Ni–SiO_2 nanomaterial.

Samples	Added (mg l^{-1})	Unadsorbed (mg l^{-1})	Extraction %
Lake water	5	0.07	98.54
	10	0.33	96.73
	15	0.39	94.07
Sea water	5	0.11	97.82
	10	0.44	95.63
	15	1.17	92.22
Tap water	5	0.07	98.68
	10	0.20	97.96
	15	0.72	95.22

3.3b *Application to real samples*: The suggested methodology was implemented for the extraction of Cr(VI) from real water samples using the standard addition method. Different environmental samples (seawater, lake water and tap water) were collected from Jeddah, Saudi Arabia. Then, the recommended procedure was applied to analyse such specimens by the above-mentioned batch conditions. Table 5 reveals that the extraction% of Cr(VI) ranged from 92.22 to 98.68%. Thus, the suggested method corroborated the suitability of the Ni–SiO_2 nanomaterial to detect and extract Cr(VI) from real water samples.

4. Conclusions

A highly selective system for Cr(VI) adsorption has been designed using the Ni–SiO_2 nanoparticles. Cr(VI) was efficiently extracted by the Ni–SiO_2 nanomaterial from aqueous solution even with the abundance of coexisting ions. The results revealed that Cr(VI) adsorption isotherm data were fitted to the Langmuir isotherm model, which suggests a

monolayer formation on the homogeneous surface of the adsorbent. Moreover, the data of the kinetic isotherm demonstrated that Cr(VI) adsorption onto the Ni–SiO_2 nanomaterial followed a pseudo-second-order kinetic model. Finally, the designed system can be effectively utilized for the removal of Cr(VI) from environmental samples.

Acknowledgements

We are grateful to the Department of Chemistry and the Centre of Excellence for Advanced Materials Research (CEAMR) at King Abdulaziz University for providing research facilities.

References

[1] Bhaumik M, Maity A, Srinivasu V V and Onyango M S 2012 *Chem. Eng. J.* **181** 323
[2] Gao Y, Chen C, Tan X, Xu H and Zhu K 2016 *J. Colloid Interface Sci.* **476** 62
[3] Kobya M 2004 *Bioresource Technol.* **91** 317
[4] Ismail M, Khan M I, Akhtar K, Khan M A, Asiri A M and Khan S B 2018 *Physica E* **103** 367
[5] Ge H and Ma Z 2015 *Carbohyd. Polym.* **131** 280
[6] Zhao D, Gao X, Wu C, Xie R, Feng S and Chen C 2016 *Appl. Surf. Sci.* **384** 1
[7] EPA 1990 *NSCEP* EPA/625/5-90/025, Cincinnati
[8] Dzyazko Y S, Rudenko A S, Yukhin Y M, Palchik A V and Belyakov V N 2014 *Desalination* **342** 52
[9] Li R, Liu L and Yang F 2014 *J. Hazard. Mater.* **280** 20
[10] Golder A K, Chanda A K, Samanta A N and Ray S 2011 *Sep. Purif. Technol.* **76** 345
[11] Dharnaik A S and Ghosh P K 2014 *Environ. Technol.* **35** 2272
[12] Hu J, Chen G and Lo I M C 2005 *Water Res.* **39** 4528
[13] Bhaumik M, Maity A, Srinivasu V V and Onyango M S 2011 *J. Hazard. Mater.* **190** 381
[14] Bishnoi N R, Bajaj M, Sharma N and Gupta A 2004 *Bioresour. Technol.* **91** 305
[15] Di Natale F, Erto A, Lancia A and Musmarra D 2015 *J. Hazard. Mater.* **281** 47
[16] Álvarez-Ayuso E, García-Sánchez A and Querol X 2007 *J. Hazard. Mater.* **142** 191
[17] Albadarin A B, Mangwandi C, Walker G M, Allen S J, Ahmad M N M and Khraisheh M 2013 *J. Environ. Manag.* **114** 190
[18] Marwani H M, Bakhsh E M, Khan S B, Danish E Y and Asiri A M 2018 *J. Mol. Liq.* **269** 252
[19] Bakhsh E M, Khan S B, Marwani H M, Danish E Y and Asiri A M 2019 *J. Ind. Eng. Chem.* **73** 118
[20] Khan S B, Marwani H M, Asiri A M and Bakhsh E M 2016 *Desalin. Water Treat.* **57** 19311
[21] Marwani H M, Lodhi M U, Khan S B and Asiri A M 2015 *J. Taiwan Inst. Chem. Eng.* **51** 34
[22] Khan S B, Rahman M M, Marwani H M, Asiri A M and Alamry K A 2014 *J. Taiwan Inst. Chem. Eng.* **45** 2770
[23] Lim M, Kwon H, Kim D, Seo J, Han H and Khan S B 2015 *Prog. Org. Coat.* **85** 68
[24] Jang E S, Khan S B, Seo J, Akhtar K, Choi J, Kim K I *et al* 2011 *Macromol. Res.* **19** 1006
[25] Khan S B, Alamry K A, Bifari E N, Asiri A M, Yasir M, Gzara L *et al* 2015 *J. Ind. Eng. Chem.* **24** 266
[26] Rahman M M, Jamal A, Khan S B and Faisal M 2011 *Superlattice. Microst.* **50** 369
[27] Khan I, Saeed K and Khan I 2017 *Arabian J. Chem.*, in press, https://doi.org/10.1016/j.arabjc.2017.05.011
[28] Dai Z R, Pan Z W and Wang Z L 2002 *J. Am. Chem. Soc.* **124** 8673
[29] Kwon S G, Chattopadhyay S, Koo B, dos Santos Claro P C, Shibata T, Requejo F G *et al* 2016 *Nano Lett.* **16** 3738
[30] Koushkbaghi S, Zakialamdari A, Pishnamazi M, Ramandi H F, Aliabadi M and Irani M 2018 *Chem. Eng. J.* **337** 169
[31] Yu J, Jiang Q, Guan Q, Ning P, Gu J, Chen Q *et al* 2018 *Chemosphere* **195** 632
[32] Gong K, Hu Q, Xiao Y, Cheng X, Liu H, Wang N *et al* 2018 *J. Mater. Chem. A* **6** 11119
[33] Shi D, Zhu G, Zhang X, Cheng M, Wu T, Zhang K *et al* 2019 *J. Alloys Compd.* **782** 183
[34] Zheng Y, Cheng B, You W, Yu J and Ho W 2019 *J. Hazard. Mater.* **369** 214
[35] Hu H, Liu J, Xu Z, Zhang L, Cheng B and Ho W 2019 *Appl. Surf. Sci.* **478** 981
[36] Khan S A, Khan S B and Asiri A M 2015 *New J. Chem.* **39** 5561
[37] Khan S A, Khan S B, Kamal T, Yasir M and Asiri A M 2016 *Int. J. Biol. Macromol.* **91** 744
[38] Ali A M and Najmy R 2013 *Catal. Today* **208** 2
[39] Han D-M, Fang G-Z and Yan X-P 2005 *J. Chromatogr. A* **1100** 131
[40] Wang L, Liu W, Wang T and Ni J 2013 *Chem. Eng. J.* **225** 153
[41] Akbari Binabaj M, Nowee S M and Ramezanian N 2018 *Int. J. Environ. Sci. Technol.* **15** 1509
[42] Krishna Kumar A S, Jiang S-J and Warchoł J K 2017 *ACS Omega* **2** 6187
[43] Gan M, Sun S, Zheng Z, Tang H, Sheng J, Zhu J *et al* 2015 *Appl. Surf. Sci.* **356** 986
[44] Zhao Y, Yang S, Ding D, Chen J, Yang Y, Lei Z *et al* 2013 *J. Colloid Interface Sci.* **395** 198
[45] Wu Y, Fan Y, Zhang M, Ming Z, Yang S, Arkin A *et al* 2016 *Biochem. Eng. J.* **105** 27
[46] Bayazit Ş S and Kerkez Ö 2014 *Chem. Eng. Res. Des.* **92** 2725
[47] Li Z, Li T, An L, Fu P, Gao C and Zhang Z 2016 *Carbohyd. Polym.* **137** 119
[48] Hassanpour S, Taghizadeh M and Yamini Y 2018 *J. Polym. Environ.* **26** 101
[49] Marwani H M, Albishri H M, Soliman E M and Jalal T A 2012 *J. Disper. Sci. Technol.* **33** 549
[50] Sharmil S R and Venugopal T 2017 *Asian J. Res. Soc. Sci. Human.* **2017** 208
[51] Freundlich H 1906 *Z. Phys. Chem.* **57** 384
[52] Langmuir I 1916 *J. Am. Chem. Soc.* **38** 2221
[53] Li Z, Chang X, Zou X, Zhu X, Nie R, Hu Z *et al* 2009 *Anal. Chim. Acta* **632** 272
[54] Wu F-C, Tseng R-L, Huang S-C and Juang R-S 2009 *Chem. Eng. J.* **151** 1
[55] Rao M M, Reddy D H K K, Venkateswarlu P and Seshaiah K 2009 *J. Environ. Manage.* **90** 634